

2019-01-01

## Development And Environmental Testing Of A Single-Axis Printer Inside A 1u Cubesat For On-Orbit Servicing Repairs In Low Earth Orbit

Perla Rocio Perez  
*University of Texas at El Paso*

Follow this and additional works at: [https://digitalcommons.utep.edu/open\\_etd](https://digitalcommons.utep.edu/open_etd)



Part of the [Aerospace Engineering Commons](#), and the [Mechanical Engineering Commons](#)

---

### Recommended Citation

Perez, Perla Rocio, "Development And Environmental Testing Of A Single-Axis Printer Inside A 1u Cubesat For On-Orbit Servicing Repairs In Low Earth Orbit" (2019). *Open Access Theses & Dissertations*. 2887.  
[https://digitalcommons.utep.edu/open\\_etd/2887](https://digitalcommons.utep.edu/open_etd/2887)

This is brought to you for free and open access by ScholarWorks@UTEP. It has been accepted for inclusion in Open Access Theses & Dissertations by an authorized administrator of ScholarWorks@UTEP. For more information, please contact [lweber@utep.edu](mailto:lweber@utep.edu).

DEVELOPMENT AND ENVIRONMENTAL TESTING OF A SINGLE-AXIS PRINTER  
INSIDE A 1U CUBESAT FOR ON-ORBIT SERVICING REPAIRS  
IN LOW EARTH ORBIT

PERLA ROCÍO PÉREZ

Master's Program in Mechanical Engineering

APPROVED:

---

Ahsan Choudhuri, Ph.D., Chair

---

Joel Quintana, Ph.D.

---

Virgilio Gonzalez, Ph.D.

---

Angel Flores-Abad, Ph.D.

---

Stephen Crites, Ph.D.  
Dean of the Graduate School

Copyright ©

by

Perla Rocío Pérez

2019

## **Dedication**

To my parents, Olga & Jose L. Pérez,

I could not have done this without your continued support through my three degrees. Thanks mom for taking care of me when I was too busy to take care of myself. Dad, thank you for helping me with my projects, I have truly been trained by the best. There are no words to thank you both, ¡gracias por todo!

To my brothers, Jose (Pepe) & Carlos,

You guys always ‘showed me off’ to your friends, I guess you made me believe I could do it. Pepe, thanks for being my personal graphic designer, my projects always looked better thanks to you.

To my extended family, my sisters-in-law America & Sara,

you have been there through it all, you have seen me at my highest and my lowest, and your support was felt.

Last but certainly not least, to my nieces, my Kami and Gissy,

may I serve as a small role model for you both so that you may be inspired to fight for your dreams. I will always be there by your side. I will always be there for you.

Again, thank you all! We did it!

DEVELOPMENT AND ENVIRONMENTAL TESTING OF A SINGLE-AXIS PRINTER  
INSIDE A 1U CUBESAT FOR ON-ORBIT SERVICING REPAIRS  
IN LOW EARTH ORBIT

by

PERLA ROCÍO PÉREZ, B.S.

THESIS

Presented to the Faculty of the Graduate School of  
The University of Texas at El Paso  
in Partial Fulfillment  
of the Requirements  
for the Degree of

MASTER OF SCIENCE

Department of Mechanical Engineering  
THE UNIVERSITY OF TEXAS AT EL PASO

December 2019

## **Acknowledgements**

I would like to thank my committee members, without whom none of this would be possible. Dr. Choudhuri, thank you for the opportunities you provide to students. I never imagined I would be working on a satellite that would be launched into space; it has been an honor. Dr. Gonzalez, thank you for being part of my committee and for your flexibility with the tight deadlines, it is greatly appreciated. Dr. Quintana, thank you for not only guiding us throughout the project, but for being there with us through the chaos. Dr. Flores, thank you for your continued patience with me and for helping me with the printer testing when I needed help. You have always been there for me and demanding great things from me; you make me believe in myself.

Thank you to all my OF-2 teammates. All I can say is, we really did it! A special thanks to Eduardo Zugasti for always taking the time to answer all my circuits questions and for programming the controller so I could continue with my testing. I appreciate the friendship we developed, and I wish you the best in your future endeavors. You are very knowledgeable in your field, thank you for allowing me to learn from you.

Thank you to all my cSETR friends, you guys have made this experience memorable. Special thanks to Lucero Buendia, thank you for cheering me on. Special thanks to Linda Hernandez; we graduated together from undergrad and embarked in the crazy journey of graduate school. Having you by my side throughout the process is the reason why I am here right now. I cannot wait to continue our journey together in Colorado.

Thank you to the cSETR office staff: Luz Bugarin, Gloria Salas, and Brenda Sanchez. What you guys do for us students cannot go unnoticed. Thanks for your support and dedication.

Finally, thanks to my best friend, Corina Lerma. I can always tell you all my struggles and you continue to provide support, and great laughs. I'm going to miss you. You're next, future Dr!

## **Abstract**

As additive manufacturing is becoming an established technology in space, new emerging strategies improve the efficiency of the printing processes. Orbital Factory 2 (OF-2) is a small satellite—or CubeSat—developed at the University of Texas at El Paso (UTEP) which launched to space on November 2019. In January 2020, it will be released in low earth orbit (LEO). OF-2 is a 1U (10x10x10cm) CubeSat that carries a one-axis printer experiment as its primary payload. This printer was developed and tested in-house. The experiment focuses on printing electrically conductive ink on a printing circuit board that verifies the conductivity on the trace once cured. This could potentially allow for the repairs of solar cells while in orbit. The printer assembly utilizes materials made from conventional additive manufacturing processes which are also space-grade to comply with space regulations, and is housed inside the chassis with the other electronic modules. Several feedbacks implemented in the design allow to track the progress of the printing process during its different stages. This paper discusses the design and development of the printer as well as the challenges and changes encountered throughout the process.

## Table of Contents

Dedication .....	iii
Acknowledgements .....	v
Abstract .....	vi
Table of Contents .....	vii
List of Tables .....	ix
List of Figures .....	x
Chapter 1: Statement of Purpose.....	1
Chapter 2: Background .....	2
2.1: Brief History of CubeSats .....	2
2.2: UTEP’s Orbital Factory 2 (OF-2) CubeSat .....	4
2.2.1: OF-2 Mission .....	4
2.2.2: OF-2 Payload Software Characterization .....	6
2.2.3: OF-2 Printer Assembly Characterization.....	8
Chapter 3: Spring-loaded Dispensing Nozzle Mechanism .....	10
3.1: Nozzle Characterization.....	12
3.2: Mechanical Testing.....	14
3.3: Electrical Testing .....	16
3.4: Integration Issues .....	19
3.5: Results.....	21
Chapter 4: Wax-Plug Sealing Nozzle Mechanism.....	22
4.1: Characterization of Wax-Plug Nozzle .....	23
4.2: Wax Static Pressure Test – FoS .....	25
4.3: Static Vacuum Test .....	27
4.4: Printer Dynamic Test .....	30
4.5: Vacuum Test .....	32
4.6: Vibration Test .....	34
4.7: Long-Term Storage.....	35
4.8: Thermal Test .....	37



4.9: Ink Cure Time .....	39
4.10: Results.....	42
Chapter 5: Solenoid Valve Nozzle Mechanism .....	43
5.1: Solenoid Valve Nozzle Characterization .....	43
5.2: Solenoid Valve Nozzle Characterization .....	45
5.3: Printer Dynamic Test .....	47
5.4: Printer Vibration Test .....	48
5.5: Nozzle Thermal Testing.....	49
5.6: Printer Vacuum Test .....	51
5.7: Results.....	52
Conclusion .....	53
References .....	54
Glossary .....	55
Vita	56

## **List of Tables**

Table 3.1: Initial burn wire test results for 30-lb strength nylon monofilament .....	16
Table 3.2: Test results for 15- and 20- lb. strength nylon monofilament .....	17
Table 4.1: Functional Testing Results Obtained from Static Vacuum Chamber Test .....	28

## List of Figures

Figure 2.1: CubeSat sizes, courtesy of NASA .....	3
Figure 2.2: CAD of OF-2 satellite assembly .....	7
Figure 3.1: Printer assembly mounted outside chassis .....	10
Figure 3.2: CAD of updated stack with printer inside chassis.....	11
Figure 3.3: Loaded and closed NC valve nozzle .....	12
Figure 3.4: Nozzle failure in original design iteration .....	19
Figure 3.5: Ink ‘backflowing’ into nozzle body during assembly.....	20
Figure 3.6: Pin stuck in nozzle.....	20
Figure 4.1: Isometric and top view of wax-plug nozzle design CADs .....	22
Figure 4.2: Rendered CAD of wax-plug nozzle design .....	23
Figure 4.3: Electrical schematic of nichrome wire connections for vacuum chamber .....	27
Figure 4.4: (a) Test setup inside vacuum chamber for static testing, (b) Deployed nozzles in vacuum chamber during static test.....	29
Figure 4.5: Updated rail CAD for bigger motor .....	30
Figure 4.6: (a) Remaining ink inside nozzle after dynamic test, (b) Test PCB with ink trace deposition and dripping.....	31
Figure 4.7: Burn wire activated during dynamic printer test in vacuum .....	33
Figure 4.8: (a) Ink deposition after vacuum chamber testing, (b) Ink deposition after two days. 33	
Figure 4.9: Vibration profile parallel to Y-axis .....	34
Figure 4.10: Vibration profile parallel to X-axis .....	34
Figure 4.11: First nozzle failure .....	35
Figure 4.12: Nozzle stress analysis from SolidWorks .....	36
Figure 4.13: N46 (left) and N44 (right) deployed during hot thermal cycle .....	37
Figure 4.14: (a) Vacuum chamber test setup, (b) Printer close-up in vacuum chamber.....	39
Figure 4.15: Conductivity test configuration (a) before the ink cures, and (b) after the ink cures40	
Figure 4.16: Ink trace deposition during ink cure time test in vacuum .....	40
Figure 4.17: Ink curing time test data in vacuum .....	41
Figure 5.1: SolidWorks drawing of NC solenoid valve printer integration.....	44
Figure 5.2: Functional testing setup of solenoid valve .....	46
Figure 5.3: Final deposition of ink during dynamic functional testing.....	47
Figure 5.4: Nozzle assembly mounted on vibration table.....	48

Figure 5.5: Cold thermal cycle setup with LabVIEW program monitoring temperature .....	49
Figure 5.6: Hot thermal cycle setup .....	50
Figure 5.7: Nozzle starting to deploy after thermal cycling .....	50
Figure 5.8: Vacuum chamber test setup (a) inside vacuum chamber, and (b) outside the chamber .....	51

## **Chapter 1: Statement of Purpose**

Technology is all around us. Every day, new technologies emerge that aim to make our daily lives easier to handle. GPS, Wi-Fi, cellphones, to name a few, are technologies we take for granted. What do they have in common? They rely on satellites. Satellites are essential on earth for communication, entertainment, tracking, monitoring of natural phenomena, surveillance, among other uses. After deployment, satellites can be operated remotely. This makes them the perfect tool for space exploration. Nowadays, the cost of sending a one pound payload into space is around ten thousand dollars. Cost can skyrocket by replacing instead of repairing. Instead of sending a new unit to space every time something is damaged, costs can be cut down by being able to repair it with something that is already in space. 3D printing has evolved greatly since its original inception. Long gone are the days that 3D printing was only used for prototyping. A myriad of materials have been developed, and many industries have been benefited by technological advancements in the field. Tools can now be printed in outer space by sending a file from the command center to the space station, an impressive feat. This itself is impressive, but what if we could use satellites and 3D printing in tandem to repair? Imagine being able to deploy a satellite with an embedded 3D printer ready to service a damaged solar cell in a matter of minutes, instead of waiting for the next shuttle deployment. An unmanned machine that can be operated remotely and used to print directly on the surface that needs to be repaired, with the ability to create a custom-made patch instead of replacing the whole cell. Several different materials have been developed since the first 3D printers, allowing for an increase in emerging technologies.

## **Chapter 2: Background**

### **2.1: Brief History of CubeSats**

CubeSats are small satellites that were first developed as a joint effort between Jordi Puig-Suari from the California Polytechnic State University (Cal Poly) and Bob Twiggs of Stanford University in 1999 to promote picosatellite development [1]. The CubeSat standard—as it became known—has allowed numerous entities around the globe to develop the small units and test new technologies in space. Various requirements that are to be followed when developing a small satellite comprise the CubeSat standard, to include: dimensional and mass requirements, structural requirements, electrical requirements, operational requirements, testing requirements, as well as other general requirements. Since the specifications have been greatly outlined to follow NASA standards, it has allowed the small satellite to grow not only at the industry level, but also at the high school and college level. A nominal 10x10x10 cm cube is what the CubeSat is designed to, with a maximum mass of 1.33kg, allowing compatibility with the Poly Picosatellite Orbital Deployer (P-POD) from which it is launched, helping cut down on costs and the reason why CubeSats are considered relatively low-cost. The CubeSat program has been successful for schools since they have a quick turn-around from planning to delivery, giving students and developers hands-on experience with space prototypes that are materialized in a period of about two years. Various companies offer commercial-off-the-shelf (COTS) ready-to-fly units and components to help with the development of the small satellites. Although the COTS components help cut down on developing and testing modules, still much effort goes behind programming the satellite to establish communication and carry out the on-board technology. The developing technologies mentioned correspond to the payload on the satellite, be it an experiment or a module developed, and are the reason for the primary mission for the CubeSat program: “to provide access to space

for small payloads” [2]. Companies and schools can obtain a flight to space by paying a sub-contractor. Schools and non-profit organizations can obtain a flight by participating in competitions and submitting proposals such as through NASA’s CubeSat Launch Initiative [3] and ULA’s CubeCorps. As CubeSats continue to develop, bigger satellite options have been since implemented. Following the same guidelines as a 1U CubeSat, bigger satellites are comprised of multiple 1U units, to include 2U’s (20x10x10 cm), 3U’s (30x10x10 cm), 6U’s (30x20x10 cm), and even 12U’s (30x20x20cm), each with varying increasing masses, respectively.

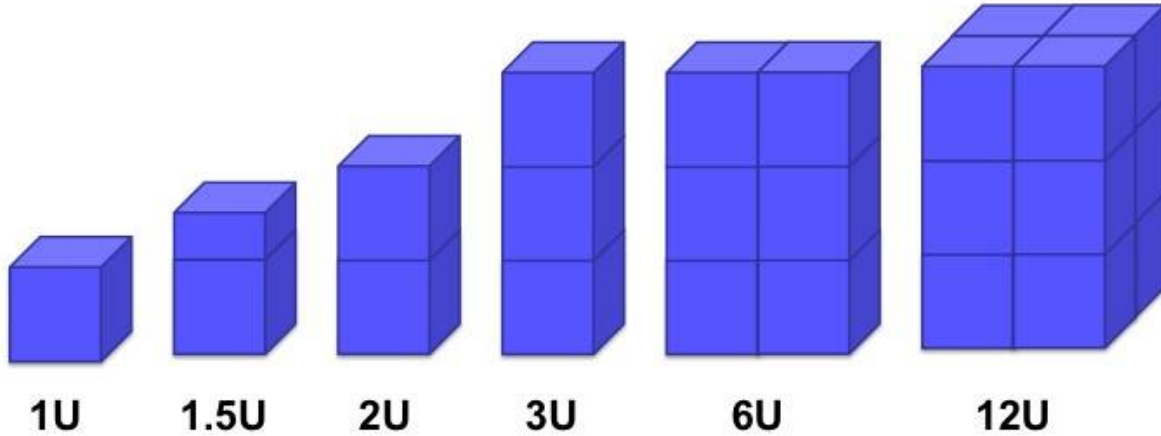


Figure 2.1: CubeSat sizes, courtesy of NASA

## **2.2: UTEP's Orbital Factory 2 (OF-2) CubeSat**

### **2.2.1: OF-2 Mission**

Orbital Factory 2 is the first CubeSat to be developed and delivered for launch by the University of Texas at El Paso. Originally set to launch in the Geostationary Transfer Orbit (GTO), OF-2 saw significant changes from its first design to its final conception, which will now be deployed in low-earth orbit in January 2020 from the International Space Station.

In 2017, a group of students from UTEP's Center for Space Exploration and Technology Research (cSETR) won the United Launch Alliance (ULA) CubeCorp competition after submitting a thorough proposal. Through the competition, UTEP was able to secure a spot on a future ULA launch mission to GTO. The center's main idea for its first CubeSat incorporated the use of a small proof-of-concept printer experiment to repair solar cells while in orbit. If a solar panel were to develop a tear, causing the system to stop functioning, the printer would deposit an ink trace on top of the tear that would become conductive upon curing, restoring the function of the panel. While all space technology is challenging to develop, an added difficulty was added by flying to GTO. More than 20,000 km above sea level, GTO experiences high level of radiation, posing a threat to the satellite and its components. To counter the radiation, the chassis was designed with a 3mm thickness all around to house the electronic modules. Following the CubeSat standard, the chosen material for the chassis was Aluminum 6061, and although aluminum is a light material, the thickness greatly affected the overall mass requirement of the satellite. The small printer assembly was housed on the outside of the chassis to prevent any damaging of the components. However, cable routing was difficult since most of all the electronics were to be housed inside the chassis.

For the first half of the development of OF-2, the mission continued to be planned for GTO. However, due to no upcoming flights to GTO until 2023, the center decided to fly through a private company, NanoRacks LLC, and leave the ULA flight for a future CubeSat, Orbital



Factory 3 which will be the continuation of OF-2. Although similar in nature, NanoRacks allowed for some changes to be made to the developing satellite.

As OF-2's mission would now be completed in LEO, the radiation was no longer a concern, thus allowing for the chassis to change to a lighter structure. This change also became an opportunity to redesign and relocate the printer experiment. Instead of mounting on the outside, the printer experiment was moved inside the chassis along with the other modules needed for the satellite. Moving the printer inside the chassis was beneficial as everything became a continuous stack. NanoRacks follows most of the design requirements used in Cal Poly's CubeSat standard, however, two differences benefitted the development of OF-2. First, the maximum mass allowed more than doubled to 2.8kg so that making changes were no longer as restricted. Also, NanoRacks deployer has a slightly different configuration, allowing for more protrusions from the x, and y faces, meaning more space could be used if desired. More changes to the satellite included the acquisition of other modules, all from the same company, to help with the communication of the satellite. The satellite was comprised of almost all COTS components from EnduroSat: UHF antenna, UHF transceiver, S-band transmitter, on-board computer (OBC), electrical power system (EPS), the 4.5 solar panels used, and the (back-up) chassis which was ultimately used. The S-band antenna was developed by Lockheed Martin and given to cSETR to test it and provide flight heritage. Lockheed Martin provided guidance throughout the development of the satellite as partnership with UTEP's cSETR. The printer experiment was developed, manufactured, and tested in-house. Two cameras, one internal and one external, also form part of the satellite. Three roller switches are utilized as inhibit switches as part of the requirements to limit the power supply to the satellite before being deployed in space.

### **2.2.2: OF-2 Payload Software Characterization**

As part of the regulations to ensure that all systems are shut down before being deployed in space, inhibit switches and a remove before flight (RBF) pin are utilized to kill power to the satellite. Once in space, the astronauts onboard the ISS will remove the pin as part of the last step before being released into outer space. The RBF pin goes directly to the EPS, thus blocking the power to the system. Although the RBF pin will be removed, the satellite will remain powered off due to the inhibit switches. Embedded along the rails of the CubeSat, the three inhibit switches—three roller switches used in OF-2—are normally-closed (NC) switches that are wired directly to the EPS as well. As the switches remain pressed along the rails of the deployer, the switch remains in the open position, and power continues to be off. When the satellite is released, it will be ejected from the deployer into orbit. Upon exiting the deployer, the switches will depress automatically and go to their NC configuration, allowing power to the system.

As the system is powered, the satellite will ‘wake up’ and all the processes will be carried out through the programmed OBC, which will power on eight minutes after deployment. A built-in 30-minute timer implemented as part of the requirements will start to run, with the UHF antenna automatically releasing once the time has elapsed. After the antenna is released, the satellite will start to beacon for a minute, allowing for communication to begin and letting the ground stations begin searching for the signal to locate the satellite in space.

Three main threads will initialize as soon as the OBC boots up: the monitor, the transceiver, and the execution thread. The monitor thread periodically logs the status of all sensors to the system log file. The transceiver thread switches UHF between beacon, transparent, and uplink mode, and inserts validated tasks into queue when received. Lastly, the execution thread continually monitors queue for tasks and executes them when encountered. Occurring in parallel with the threads are the printer experiment, the S-band experiment, as well as the extended mission.

Printer operation is carried through a microcontroller which runs the motor through I2C communication. An inward camera will take continuous pictures to track and document the printer

experiment throughout the different stages. Five stages are followed in the printer operation. First, the OBC receives the status from the homing mechanism. By doing this, the controller verifies the position of the printer by checking with predefined logic. At the second stage, if continuity of not detected from homing mechanism, the nozzle will begin to move to the initial position. Third, once 'home', a picture of the initial conditions at the beginning of the experiment is taken. Here, the temperature sensor verifies optimal conditions for printer operation. In the fourth stage, the nozzle mechanism is activated while the motor is powered on to begin depositing the ink on the test PCB. After three minutes, at the last stage, the conductivity in the PCB board is checked, and another picture is taken to see the changes during the experiment. After that, the printer experiment ends.

Universal Asynchronous Receiver Transmitter (UART) serial communication is used by both cameras which are controlled by the OBC. With a higher resolution, the outside camera saves the packets in large files. To minimize downloading time, low-resolution images will be downloaded first at around 70 packets and a download time of 5.5 minutes, downloadable in one pass above the ground station. Thus, if the picture is not pointing somewhere optimal, then the high-resolution picture will not be downloaded on future passes. Since the UHF transceiver communicates most mission data with the ground, the continuous mission aims to receive additional files and updates, new commands to have a programmable CubeSat in orbit, kill signals, etc. If the S-band antenna is successful, faster downlink would allow for the picture packages to be obtained by the ground station.

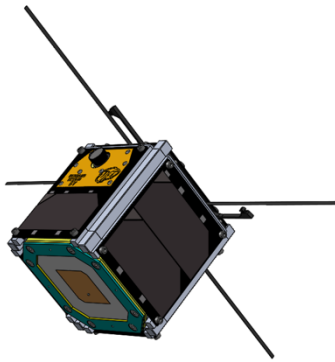


Figure 2.2: CAD of OF-2 satellite assembly

### **2.2.3: OF-2 Printer Assembly Characterization**

Even through the design changes made to the printer, the overall mechanism has remained unchanged. For the proof-of-concept experiment, the printer assembly remained a one-axis printer that would move side to side to deposit an ink trace on top of a PCB. From its inception, there were certain requirements that may have restricted the design, ultimately setting up the boundaries around which to conceptualize the design. With the idea that the printer experiment embodied concepts of 3D printing, selective laser sintering (SLS) and conventional fused deposition model (FDM) were utilized to manufacture some components of the printer assembly. The mounting rails were printed conventionally out of ULTEM 9085, and the nozzle was SLS printed out of ProtoTherm 12120. Both materials selected are materials approved for space use based on NASA's outgassing requirements. Also, both components were printed by the W.M. Keck Center at UTEP. Since the parts could easily be changed using CAD software, it proved beneficial to use these additive manufacturing methods and obtain customized parts in a relatively quick turn-around period.

Utilizing the PC/104 architecture, the ULTEM rails serve as the main structure for the printer assembly. By having them separated, the two rails help in bringing the assembly together. Embedded on one of the rails is the stepper motor, which is connected to a threaded rod through a coupling. The threaded rod passes through a small hex nut epoxied inside a small aperture on top of the nozzle. To keep the nozzle from spinning 360° in the same place, a couple of metal rods also pass through the top of the nozzle and are used as guides. Thus, the nozzle can move left and right when the motor is activated. The conductive ink is housed inside the nozzle assembly, or simply nozzle, and has its own deployment mechanism. A test PCB sits in front of the nozzle tip at a separation of .5mm, enough distance to allow the ink to come out be deposited on top of the PCB. Two grooves on the mounting rails hold the test PCB in place, and the test PCB has a surface mount that connects to the PCB controlling the whole experiment. Several test points on the test PCB will determine if the experiment has been successful. The circuitry on the PCB is not

continuous—the conductive trace is what connects the test points on the board and creates the continuity. After the ink is deployed on it and after the ink has cured, the OBC will check for conductivity at the different test points. This means that although the idea is to deposit a continuous trace, the experiment will be successful if continuity is detected between any two test points.

One of the greatest restrictions in the design of the printer assembly was to design in the limited space available in the satellite. The printer experiment, although the primary payload onboard the satellite, was one of various modules needed in the CubeSat. The limited space is one of the reasons why the printer is only one-axis. Any change in the printer design was first modeled in CAD to see about any interference with the rest of the satellite.

Tasked with hardest job in the experiment, the printer nozzle assembly was the one to see the most changes. Through every design there were three important tests to keep in mind to comply with the CubeSat requirements: vibrate test, thermal test, and vacuum test. During launch, the satellite encounters intense vibration, and the satellite needs to survive it. No part of the satellite, including the components inside, should break, as they may pose a risk and/or cause space debris. Also, the temperature in space varies greatly and thus, the experiment should be able to perform at any given temperature. A temperature range of  $-40^{\circ}$  to  $60^{\circ}$  C was provided by NanoRacks, and the testing was done at those limits although most of the temperature would affect the outside of the satellite more directly due to there not being convection in space. Nevertheless, testing at the limits provides testing at the worst-case scenario. Lastly, the printer experiments were successful if it could work, but space environment is extremely different. Testing the printer experiment inside a vacuum chamber gave insight into the behavior of the printer in more realistic space conditions. Due to the testing requirements, the printer assembly, especially the nozzle, was subject to three main design iterations to ensure the functionality of the system in space, and passing the three main tests. More information on the design changes continue in the chapters to follow.

### Chapter 3: Spring-loaded Dispensing Nozzle Mechanism

Orbital Factory 2 was preliminarily going to be deployed in the Geostationary Transfer Orbit. Due to the radiation there, the 1U chassis consisted of thick aluminum walls to allow the satellite to survive at least for five days, the duration of the mission. To prevent any ink spillage from affecting the electronic modules, the printer was isolated outside (Figure 3.1). Standoffs stabilized the printer and the nozzle rested on 3D printed rails that served as a gantry mechanism

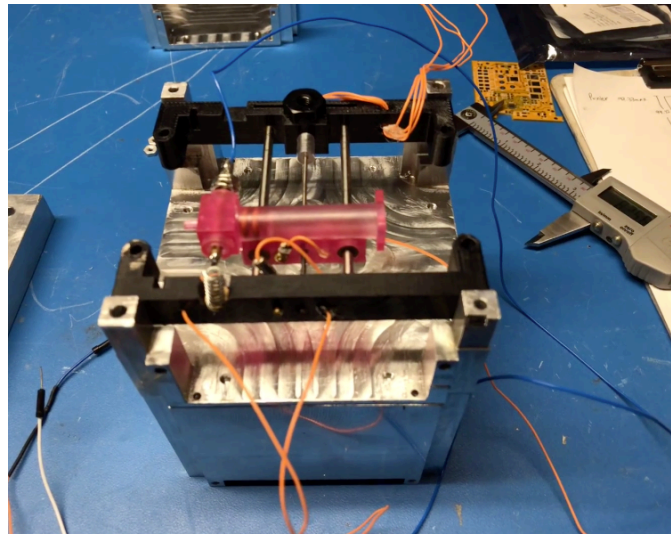


Figure 3.1: Printer assembly mounted outside chassis

for the printer. A spring-loaded dispensing nozzle mechanism housed the ink to be deployed during the experiment.

Most of the testing performed on the printer design was devoted for testing the conductive ink itself, which ultimately allowed for the Ercon E1660 ink to be chosen and defined as the best alternative for the on-board experiment [4]. However, limited information on the printer design itself led to the need of characterizing and testing the printer design.

A change in the mission prompted the first changes in the overall design. As the satellite would now be launched in low-earth orbit (LEO), the design of the chassis was changed to have thinner walls, bringing down the weight of the chassis. Two cameras were also added to the design, one to take pictures inside during the experiment, the other facing outside to take pictures of the

Earth once deployed. Moving the printer mechanism inside the chassis with the other modules allowed for easier cable routing as well as the ability to use the PC-104 architecture to stack the printer along with the rest of the components (Figure 3.2).

As the printer sat on top of the modules, a Kapton enclosure would be added to mitigate any risks associated with ink spillage. The Kapton would go around the main structure of the printer, enclosing the rails and thus only covering the printer itself, without including the PCB with microcontroller used in running the printer.

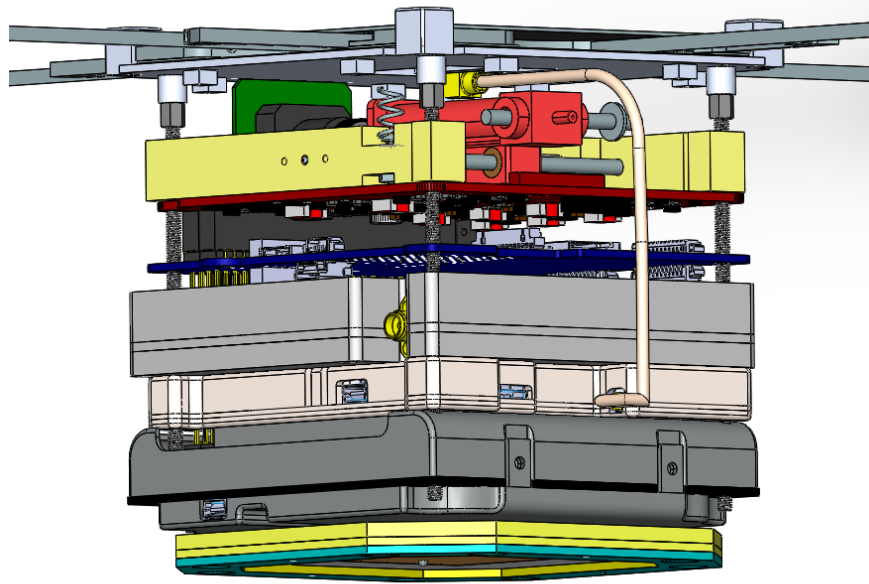


Figure 3.2: CAD of updated stack with printer inside chassis

### 3.1: Nozzle Characterization

As a preliminary concept, the nozzle design used in the testing of the ink resembled a normally closed (NC) valve that would dispense the ink until the mechanism was activated. Two springs were utilized to control the mechanism: one to open the spring-loaded valve, and another for the spring-loaded piston that would push the ink out onto the test PCB. A compressed spring inside the nozzle body meant that the nozzle was always pressurized, leaving the NC valve with the task of holding the ink inside until the experiment would be conducted. Silicone O-rings were used to seal the openings where ink might escape: around both ends of the pin, and embedded in the pusher inside the nozzle body. Figure 3.3 shows the design of the NC spring-loaded

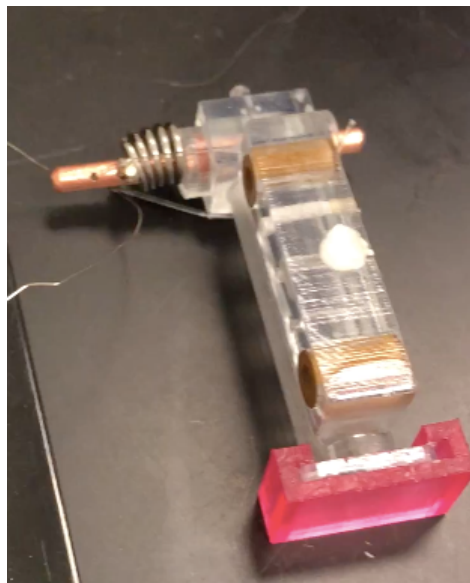


Figure 3.3: Loaded and closed NC valve nozzle

dispensing nozzle mechanism when loaded with ink. When closed, the copper pin at the front of the nozzle would stop the flow of the ink. In this closed position, the pin also served as a homing mechanism during the programmed printer instructions. During the printer sequence, the nozzle first moved towards a designated homing position at the rightmost of the rails. When the nozzle was closed, the protruding pin would touch a feedback system embedded in the mounting rails, creating continuity and confirming the position of the printer at the beginning of the experiment.



Nylon monofilament held the NC valve mechanism closed by keeping the spring compressed. Type C Nichrome was used as burn wire and was wrapped around the nylon cord. Once the experiment started, voltage was passed through the burn wire, causing it to heat up quickly, eventually melting the nylon cord which forced the valve mechanism to open. The spring would decompress, forcing the pin to move out. This intricate mechanism was carefully tested, as a small groove on the pin had to align with the nozzle tip to serve as a channel for the ink from the nozzle body (where the ink was stored), to the tip of the nozzle. As the valve opened, the moving pin would also break the continuity of the feedback system. At this point, the system would see this change and begin moving the printer to deposit the ink on the PCB.

### **3.2: Mechanical Testing**

Learning the mechanics of the NC valve nozzle was not difficult to understand. However, attempting to figure out what components were used in the printer the assembly and why those components were selected, took more time to understand. As stated before, little documentation on the proceedings of the nozzle design led to a need to characterize and test the nozzle to ensure functionality and reliability.

As a first step, the components of the nozzle were procured to test the mechanical functionality of the NC valve system, with no ink. With the design of the nozzle fixed, the length of the pin was determined by only having the smallest amount of copper pin utilized. Thus, a size of 38.5mm was selected, enough to stick out of the nozzle and touch the homing mechanism when closed, and long enough to fit the spring on the other side when opened and still covering the inside portion of the nozzle to serve as the channel for the ink to pass through. Two small holes were drilled close to one of the ends of the pin and were also subjected to accuracy errors. The outermost opening was only used to tie the nylon string and burn wire to the nozzle body. On the other hand, the second opening was used to place a smaller pin (3/16" diameter) through the pin and soldered in place to work as a stopper for the spring. Solder works better with certain metals such as copper, thus the reason for choosing the copper pin in the assembly.

For such a small and intricate system, tolerances quickly stacked up and posed certain risks. Human error was introduced when cutting the springs used to open the nozzle and when drilling the two smaller holes through the pin. It was essential to be pay close attention to the mechanism and ensure the opening in the pin aligned with the nozzle tip once the valve was activated so that the ink could flow through the channel. This opening was a small aperture closer to the other end from the spring. A simple way to reduce the risk of the pin blocking the opening even when the valve was activated was to make the aperture in the pin a little wider. A .8mm diameter was the measurement of the nozzle tip, which is why the tolerances were concerning, so adding a little more space on the side of the measured opening proved beneficial to the design.

To test the functionality, the nozzle NC valve system would be assembled, with the only missing component in the assembly being the conductive ink and burn wire. A pair of wire cutters was used to cut the nylon monofilament to activate the valve mechanism. Since the nozzle material is semi-transparent, it was easy to see if the groove on the pin would align with the nozzle tip once it opened. Once several tests confirmed the functionality, then it was tested with the burn wire mechanism.

### 3.3: Electrical Testing

Instead of using cutters, the Nichrome wire was added to heat the monofilament and break the line. While adding the burn wire was easy, it quickly became obvious of the importance of placing the wire correctly. Both the nylon and nichrome were passed through the same orifice; however, the nylon was tied against the body of the nozzle while the nichrome was connected to power. Braiding the nichrome under the nylon three times with a snug fit became the best way to ensure optimal contact between the two.

A power source was used to provide 5V to a breadboard, corresponding to the voltage allocation from the EPS in the satellite. One end of the burn wire was placed in the positive, while the other end was placed in the negative terminal. The power supply was powered on and after a few seconds, the NC valve nozzle would open. Preliminary time measurements were gathered to see how long it took for the nylon to break, as recorded in Table 3.1 below. Initially, a nichrome

Table 3.1: Initial burn wire test results for 30-lb strength nylon monofilament

<b>Nichrome wire length (cm)</b>	<b>Supplied Voltage (V)</b>	<b>Recorded Amperage consumption (A)</b>	<b>Time recorded to break monofilament (s)</b>
9.5	5	2.2	2
13	5	1.5	8.5

monofilament with a strength of 30 lbs. was used to hold the nozzle together, and a 30 AWG Nichrome wire, both of which had been left behind as part of the design.

An immediate concern was raised by the amperage utilized by the burn wire. A maximum of two amps was the maximum amount handled by the EPS. Due to this, different strength nylon wire and different size nichrome wire combinations would be tested to minimize the amperage utilized. Nylon wire with less strength meant that the diameter of it was smaller, which translated into less time that the burn wire had to be used. The 30-lb nichrome had a diameter of .023", the

20-lb a diameter of .0185”, and the 15-lb one a diameter of .015”. A summary of the results is displayed in Table 3.2 below. When testing the different strengths, the nozzle assembly was

Table 3.2: Test results for 15- and 20- lb. strength nylon monofilament

<b>Nylon strength (lbs.)</b>	<b>Nichrome wire length (cm)</b>	<b>Supplied Voltage (V)</b>	<b>Recorded Amperage consumption (A)</b>	<b>Time recorded to break monofilament (s)</b>
20	13	5	1.7	2.5
	16	5	1.48	7
	18	5	1.4	8
	20	5	1	Did not break
15	13	5	1.7	2.76
	16	5	1.42	2.89
	16	5	1.37	4.25
	16	5	1.4	3.26
	18	5	n/a	Did not break

utilized, ensuring that the nylon would be hold the nozzle in the closed position. Based on this, a nylon wire with a strength of 6-lbs was discarded. Due to its thin diameter of .010 in, the nylon could not be wrapped around the nozzle body fast enough to hold it together with a series of knots. Although only two other nylon strengths were tested, the combination of 15-lb strength nylon with a burn wire length of 16 cm obtained good results. With the highest amperage consumption of 1.42A, and a maximum time of 3.26s for the nylon to break, it fell under the stipulated limit while also keeping the burn wire running time to a minimum. The length of the burn wire was also easy to work in the assembly. Keeping in mind that the printer assembly would be placed inside the

CubeSat, a shorter burn wire length was preferred to minimize the burn wire heating up and/or damaging other components, especially in the tight space the printer was allocated.

With the nozzle mechanism fully functioning, the next part became to test the fully assembled nozzle, including the ink.

### 3.4: Integration Issues

The last step in the testing of the nozzle was to add the ink to the nozzle assembly. Integration issues were seen from the beginning as though the valve was in the closed position, ink was leaking through the nozzle tip and through one of the sides where the pin was located, as shown in Figure 3.4. Since the nozzle was not sealing properly, changes needed to be made. To



Figure 3.4: Nozzle failure in original design iteration

reduce the number of changes and taking into consideration the components used that are in-stock, changing the pin diameter was not considered. The pin and O-rings combination were compatible with each other. Thus, modifications were made to the CAD of the nozzle to decrease the pin hole diameter, and to reduce the diameter where the O-rings sat to create a tighter fit. As different batches of printed nozzles were tested, the leakage would be less, but sometimes when loading the nozzle with ink, the ink would leak into the nozzle body itself, as in Figure 3.5. This could be fixed by making the ink pusher a bit bigger to also create a snug fit with the O-rings utilized embedded in it.

As the diameter of the pin whole became smaller, the leaking was diminished but it was harder for the spring to move the pin when opening the valve. The diameter was changed to one so small that the issue of leaking was no longer a problem, however, the nozzle was not even tied with nylon to keep close, and even with the spring compressed, exerting force for the pin to move,

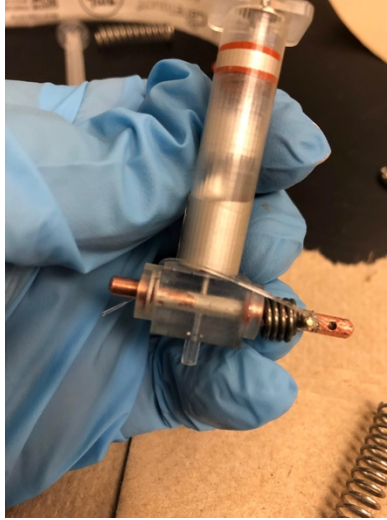


Figure 3.5: Ink ‘backflowing’ into nozzle body during assembly.

the nozzle remained closed (Figure 3.6). With the tight fit, it was also harder for the ink to be loaded as it was so air-tight that the ink pusher could not be moved down to the bottom, in certain circumstance. No combination of pusher and pin hole diameter seemed to resolve the issues with the nozzle.



Figure 3.6: Pin stuck in nozzle



### **3.5: Results**

Environmental testing could not be performed until the nozzle was working properly. As the nozzle mechanism and its issues began to be characterized, several concerns were raised during the nozzle integration. Slowly, the integration issues were starting to be resolved and more analysis could have been done to find the appropriate spring that would open the valve, and perhaps find a different method to load the ink. Repeatability and reliability were essential, both of which the current design was lacking. The complexity led to many points of failure, and the risks implied were not ready to be undertaken. Due to the intricate design and accompanying complexity, a simpler solution was sought to ensure functionality.

## Chapter 4: Wax-Plug Sealing Nozzle Mechanism

A redesign of the nozzle was needed to keep advancing in the testing of the printer. Various ideas were considered and discussed, all with the goal to have a simple design. Remembering that the nozzle was always under pressure, the second design emerged from only needing a plug to keep the ink from coming out. Furthermore, the addition of a wax plug was considered and explored. Used in space applications, the new wax plug mechanism was designed and tested. Figure 4.1 shows the CAD of the simplified nozzle assembly.

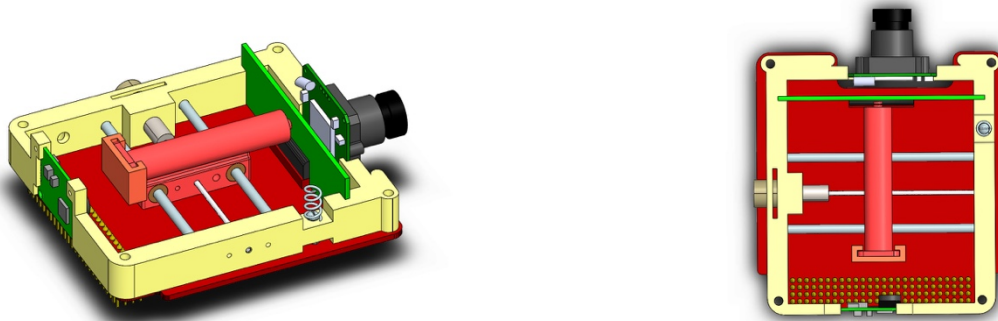


Figure 4.1: Isometric and top view of wax-plug nozzle design CADs

#### 4.1: Characterization of Wax-Plug Nozzle

Adding the wax plug meant that the nozzle design was greatly simplified. The spring-loaded pin mechanism serving as the NC valve was removed so that the nozzle became mostly a cylinder with a nozzle tip at the front.

To add the wax seal, wax was melted on a small container such as a metal lid, and the tip of the nozzle was dipped in the wax. After sealing the nozzle, the other components would be added the same way as before (ink, ink pusher, spring, end endcap). Just as with the previous design, the nozzle was always pressured due to the spring inside the nozzle body pushing on the ink pusher. Nichrome wire was kept and this time utilized to melt the wax. It was placed close to the tip of the nozzle so that when voltage was passed through the burn wire, it would heat up, consequently heating up the nozzle and eventually melting the wax. As the wax melted, it would be unable to hold the pressure and spring would begin to push the ink out from the tip. Once the wax melted, the motor would start turning so that the ink trace could be formed on the test PCB.

After a few tests (to be discussed in the following sections), a ridge around the nozzle tip was implemented to keep the burn wire in place. This increased the chances of the burn wire to remain attached to the nozzle tip even through the vibration launch environment.

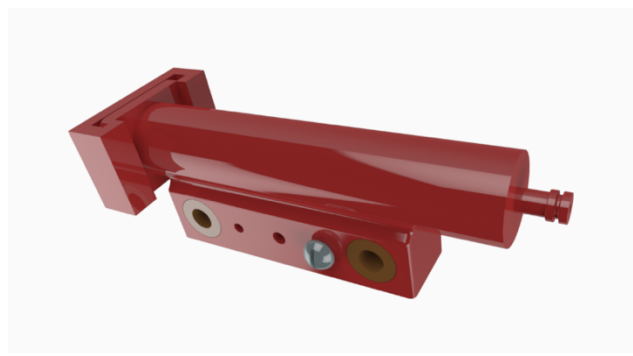


Figure 4.2: Rendered CAD of wax-plug nozzle design

In general, the design of the printer remained virtually the same, with the big change being in the nozzle itself. With the removal of the pin, however, the feedback system indicating when the nozzle had opened was eliminated. The pin was key in determining when the ink started

flowing so that the motor could start moving. The home switch mechanism remained unchanged and could still be used to move the nozzle to the homing position. Both cameras remained in the assembly as well.

## 4.2: Wax Static Pressure Test – FoS

Before conducting other tests, the first step was to check if a wax plug could hold the ink inside in the pressurized nozzle. In procuring a high melting point wax, the IGI 4621 paraffin wax with a melting point of 142°F (61.1°C), and the IGI 4641 paraffin wax with a melting point of 163°F (72.78°C) were both chosen because their melting points were higher than the upper limit of the mission temperature. The IGI 4621 is referred to as the low-melting point wax (LMPW), and the IGI 4641 as the high-melting point wax (HMPW). To accelerate testing, however, a regular candle was used to perform some preliminary tests and gain insight into the new ink deployment mechanism while the wax arrived.

When loading the nozzle with 1mL of ink, the spring would compress different lengths due to the air that was introduced in the system. As the nozzle was sealed and then the ink and ink pusher were introduced, sometimes the ink pusher would not go all the way to the bottom. Even with the ink pusher pushed manually, it would not go all the way down. Several measurements were recorded and the maximum spring displacement was recorded, corresponding to the highest pressure introduced in the system. With an original length of 1.375", and a spring rate ( $k$ ) of 5.18 lbs./in corresponding to spring #4047 (part number), the maximum spring displacement occurred at  $x=.8125$  in. Using Hooke's law,

$$F = -kx$$

the force exerted by the spring was ~4.21lbf. To obtain the pressure exerted, the pressure formula

$$P = \frac{F}{A}$$

was used. The force is exerted by the spring to the back of the ink pusher, which is roughly the size of the inside of the nozzle. To calculate the area, the formula for the cross-sectional view of a

circle was utilized, with the diameter being 8.9mm or .35in. The pressure calculated was 43.74psi, which was about the maximum pressure observed inside the nozzle.

Using a simple setup, a couple of nozzles' tips were submerged into the wax. A height of  $\sim 1/16$ " of wax was observed to have gone inside the nozzle tips. An air compressor with a silicone tip (providing some sealing between the surfaces) was introduced to the back of the nozzle to simulate the pressure inside the nozzle. Slowly, the pressure of the air compressor was raised up to 7 bar,  $\sim 101.53$  psi. At that pressure, the Factor of Safety (FoS) was of at least 2.32. Since the simple setup was not designed for a burst test, the results were only used to ensure that the wax plug could hold the ink. Although there was no air escaping from the nozzle tip throughout the experiment, the nozzles were submerged under a clear cup of water to see if any bubbles formed, but no bubbles were observed in either case. Thus, the first test had been a success.

### 4.3: Static Vacuum Test

Continuing with the preliminary tests, a series of nozzles were tested with the nichrome wire to see if it would melt the wax. Because the wax was at the nozzle tip, the burn wire was also placed close to the tip. Using a pretzel knot, the nichrome was tied as snug as possible on the tip. However, the wire could move in and out of the nozzle tip if it was accidentally pulled with not much force, thus the later addition of the ridge at the end of the nozzle tip as mentioned earlier.

With the nichrome wire able to melt the wax, the system was then tested in vacuum to see the viability of its use for the experiment. Two nozzle assemblies were utilized for the test. The loaded nozzle assemblies were each labeled and taped onto an acrylic sheet. Nichrome wire cut to 16cm was then wrapped around each nozzle tip, and each of the ends of the wire were connected to alligator clips to the vacuum chamber's connections. On the outside of the vacuum chamber, the connections led to the positive and negative of the power supply.

Once the setup was complete, the vacuum chamber was powered on. Throughout the testing, the vacuum chamber was constantly being monitored through its small window opening. From rough vacuum to high-vacuum ( $\sim 10^{-5}$  torr), the nozzles were observed to ensure there was no leakage at the tip of the nozzle, or at the back of the nozzle plunger. It was observed that both nozzles survived in high-vacuum as the ink remained inside the nozzle until the burn wire was activated to melt the wax. Upon reaching high vacuum, the nozzle assemblies were tested

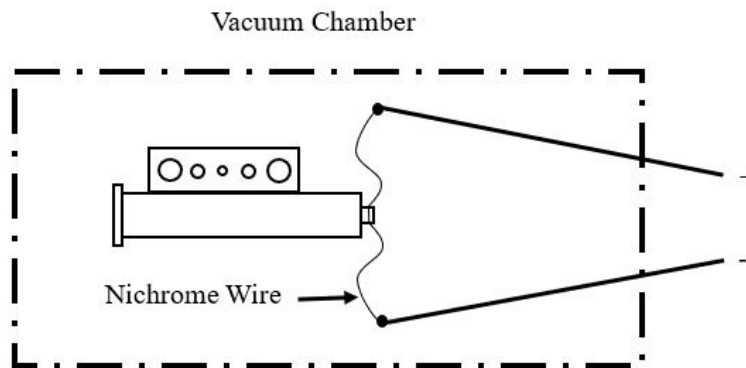


Figure 4.3: Electrical schematic of nichrome wire connections for vacuum chamber

separately. The correct connections for that nozzle were plugged to the positive and negative terminals of the power supply (Figure 4.3). To reduce the amperage consumption, the current was limited to 0.3A, while the voltage was left at 5V. The results of the test can be observed in Table 4.1 below. When the burn wire was activated, the voltage on the power supply changed to 1.3V,

Table 4.1: Functional Testing Results Obtained from Static Vacuum Chamber Test

Nozzle Identifier	Visible leaks before activating burn wire?	Time (s) to melt wax plug?	Ink released?	Operating voltage observed in power source?
N5	N	42	Y	1.3 V (at 0.3 A)
N6	N	45	Y	

the operating voltage. This was explained through Ohm's law, as  $V = IR$ . Since the current was limited, the only other factor that could change was the voltage, as the resistance was dictated by the burn wire. The operating voltage for the experiment was .39 Watts ( $1.3V * 0.3A$ ). Accounting for the longest time taken to release the ink (45s), the power consumption  $P = .39W * 45s = .004875W*hr$ .

In both cases the ink survived high vacuum and all the ink was completely pushed out of the nozzle. Due to the nature of the static test, the ink accumulated at the tip of the nozzle, forming a bubble of ink on the acrylic.



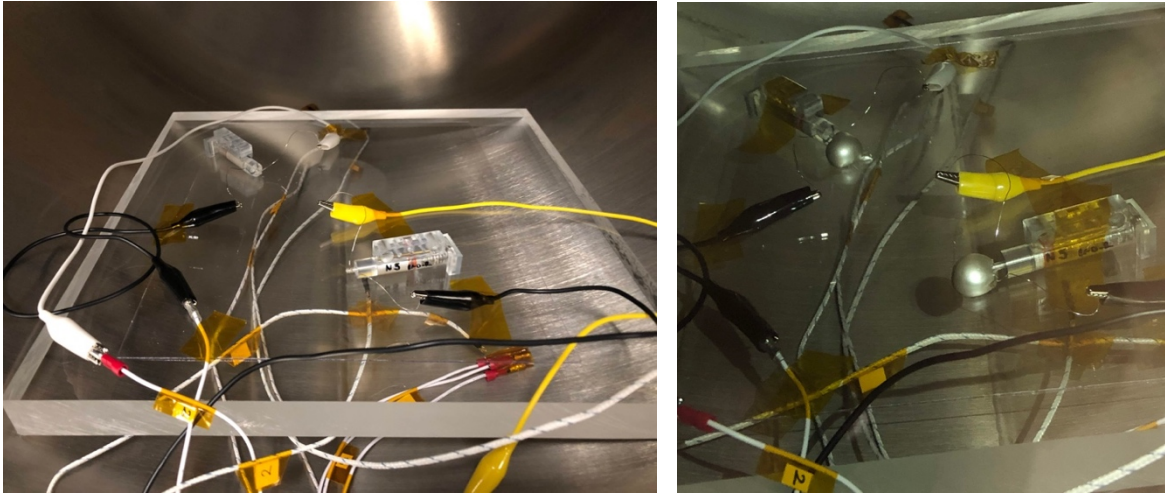


Figure 4.4: (a) Test setup inside vacuum chamber for static testing, (b) Deployed nozzles in vacuum chamber during static test

#### 4.4: Printer Dynamic Test

Still awaiting the wax, the next task was to work with the rest of the printer assembly and be ready to conduct dynamic tests. The next step was to assemble the printer completely including the wiring system. As the printer control board was still under development, the motor testing was controlled with an Arduino. At first, only the movement of the nozzle was taken into consideration; the nozzle was not loaded for the tests. Overall, the nozzle was moved using the motor, but issues were experienced during the movement. In some instances, the nozzle would get stuck and would stop moving. If it did move, it was not a smooth movement. If a wire from the printer assembly got in the way of the nozzle, it would get stuck. An analysis had initially been done when the motor was selected, but most likely any imperfections in the system were not considered. Some of the issues why the motor was getting stuck was due to a bent threaded rod during cutting and handling. A newer threaded rod was used, but the issue of any connection getting on the way of the nozzle was still concerning. Also, the threaded rod could get bent during the launch environment. Taking the concerns into consideration, a bigger motor with a higher torque was selected. While no major changes were introduced, some adjustment needed to be made in the motor rail, as seen in Figure 4.5. A cutout in the printer control board had to be implemented for the motor to fit.

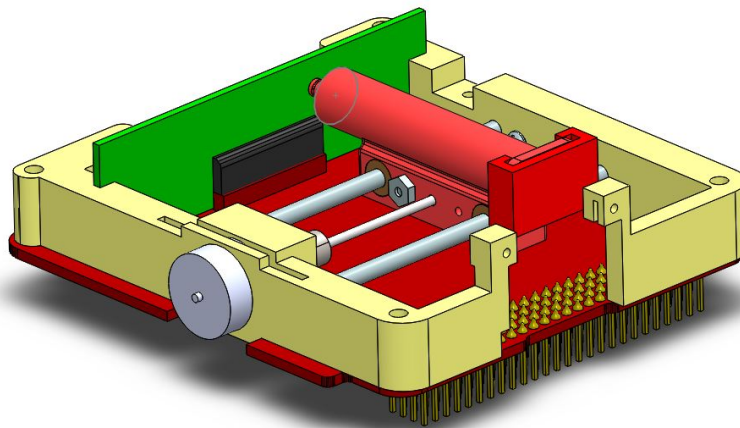


Figure 4.5: Updated rail CAD for bigger motor

Still utilizing the smaller motor, a dynamic test was performed. Using the same set up as before, the Arduino was programmed to be moved with two buttons, one to go to the left and the other to go to the right. Thus, the experiment was visual and controlled by hand. Upon melting the wax with the burn wire and ink started coming out, the button was pressed to move the nozzle. On the first pass, there was a break at the beginning of the print. The ink started coming out and the nozzle was moved, but then it took a second for ink to start coming out again. Passing the nozzle back and forth a couple of times helped spread the ink onto the test PCB. A total of two passes completed the experiment (left, right, left, right) to end at the homing position. When the test was completed, there was more than half the ink left inside the nozzle still. With the nozzle resting at the homing position, the ink kept slowly coming out and dripping onto the board. Loading the nozzle with less ink was a simple solution to prevent any ink run off.

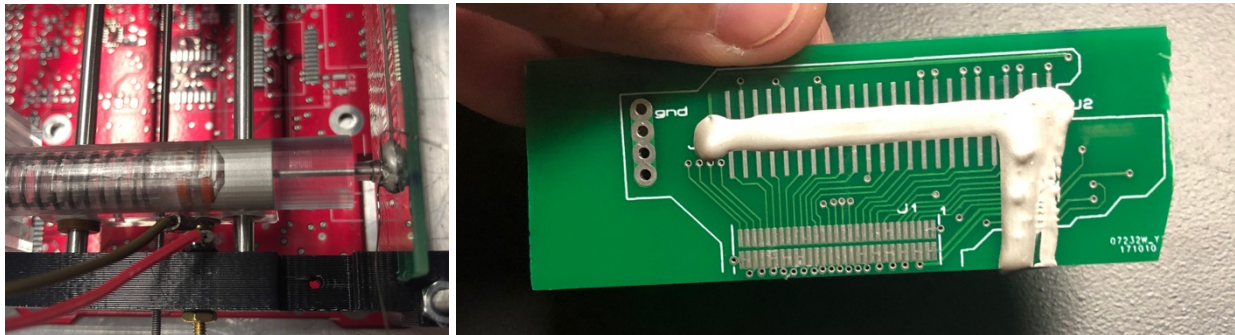


Figure 4.6: (a) Remaining ink inside nozzle after dynamic test, (b) Test PCB with ink trace deposition and dripping

During the test, the burn wire was activated for 17 seconds, with a power consumption of 5V at 1.35A. These were unexpected results from the nichrome burn time, and more testing was needed for repeatability.

#### 4.5: Vacuum Test

Vacuum chamber testing was conducted to see the performance of the dynamic printer assembly while in vacuum. The test would be used to validate that the wax seal can contain the ink, to validate the success of the burn wire, and to test the dispensing of the ink with a moving nozzle in vacuum. The set up from the previous printer dynamic testing would be utilized, with the autonomous program being tested, with the only input being starting the experiment after visual conformation of the wax melting (ink starts coming out). A watershed nozzle with 2.10mm HMPW plug was utilized, loaded with 0.6mL of conductive ink. Success criteria was identified for the testing, keeping in mind that the experiment would be completed while inside the vacuum chamber which could not be interrupted mid-operation. The success criteria were heavily based on the observations made through the vacuum chamber window and are summarized as follows:

1. The nozzle assembly must remain closed, with no leaks, from the beginning of the experiment to high-vacuum. No ink should be seen coming out of the nozzle tip and/or inside the nozzle body itself.
2. Once activated, the burn wire will be successful if it is able to melt the wax and allow for the ink to flow through.
3. The ink should be completely dispensed, which will be seen due to the transparent color of the nozzles in the watershed material. If not completely dispensed, there should not be any ink ran-off which might affect the other components.
4. A consistent trace should be placed on the test board.

Ideally, the criteria would be met one by one, and when the 4 were met, then the OF-2 nozzle would work dynamically in vacuum.

To begin the experiment, the burn wire was powered at 5V for 16s, pulling 1.20 Amps. After the experiment was carried out, the results were as expected. The nozzle sequence was performed with no issues. When the motor stopped, the remaining ink inside the nozzle did start congregating at the tip, however it did start dripping as it had done before in atmosphere testing.



Figure 4.7: Burn wire activated during dynamic printer test in vacuum

Even though the vacuum chamber was turned off at the end, the assembly was left inside for a couple of days. Checking in afterwards, all ink had eventually made it out of the nozzle but the ink did not leak onto PCB. Instead, it congregated at the nozzle tip and cured.

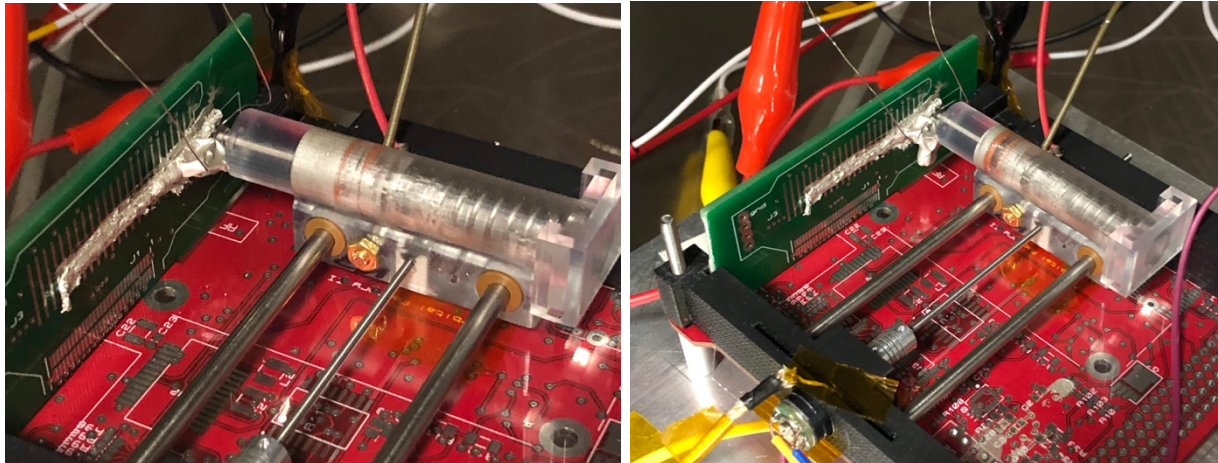


Figure 4.8: (a) Ink deposition after vacuum chamber testing, (b) Ink deposition after two days



## 4.6: Vibration Test

To conduct the vibration test, the printer assembly was mounted on top of an aluminum plate used when assembling the printer. The test would be used to ensure the wax plug would not be damaged during vibration. No wiring was included in the printer assembly. For the preliminary test, only the X- and Y- axis orientations were tested.

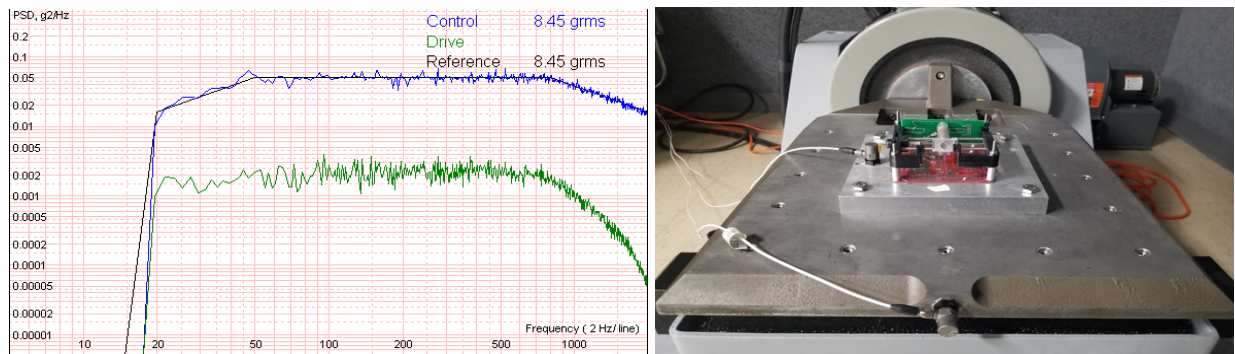


Figure 4.9: Vibration profile parallel to Y-axis

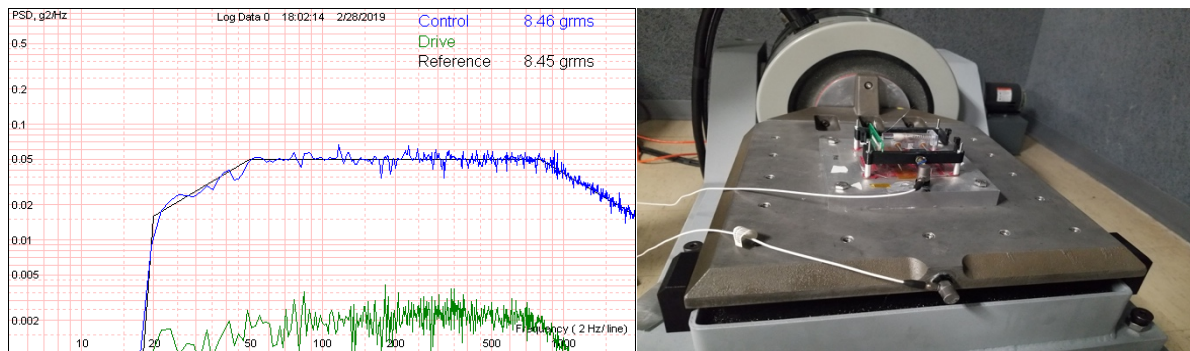


Figure 4.10: Vibration profile parallel to X-axis

Two accelerometers were used per axis, one placed on the test element plate and the other placed at the edge of the shaker table, thus the colored lines in the graphs. The solid black line is the profile programmed on the vibration table (to coincide with NanoRacks vibration profile).

After the vibration test, the printer assembly was inspected carefully. The only visible damage was the loss of cable tubing on the motor. The nozzle, however, remained sealed even after the test.

#### 4.7: Long-Term Storage

An implied requirement for the printer assembly was that it had to survive for a period of 3-4 month before conducting the experiment in space. The satellite would be delivered in September where it would be mounted inside the deployer. Then, the satellite would be launched into space in October, remaining outside the ISS until January 2020. Thus, a simple test for long-term storage was done. Nozzles were loaded with ink and left inside a cabinet. Besides the required amount of time in storage, the test emerged from an incident with one of the nozzles. A previous nozzle used in early testing where too much wax was added (and could not be melted) was left in storage. That experiment had occurred in January 16<sup>th</sup>. On February 19<sup>th</sup>, the nozzle was burst. Most of the ink was fresh so it had happened within one or two days prior as the ink takes longer to cure at atmosphere. The fresh ink also indicated that the ink had cured and expanded. Revisiting the safety data sheets, there was no mention of any reactivity between the ink and the plastic. The ink itself is stored in plastic containers. Only about 4 to 5 weeks had passed between the assembling of the nozzle and its failure. Two other nozzles intended for storage also failed at the 5-week mark.



Figure 4.11: First nozzle failure

While there was no clear answer as to what was causing the failures, it was attributed to creep. It is important to note that most of the testing was done using watershed nozzles due to the turn-around time in manufacturing. Although similar, ProtoTherm nozzle is stronger than the

watershed, and it is also the one that is used in space applications. A simple SolidWorks simulation confirmed that ProtoTherm should withstand the pressure exerted from the spring. Using the highest calculated pressure from before (43.74psi) and applying that to the inside of the nozzle, the maximum von Mises stress was  $3.118 \times 10^6$  Pa ( $\sim 452.2$ psi) which is less than the 70.2MPa tensile strength of the material. With no anticipated problems with the ProtoTherm nozzles, the

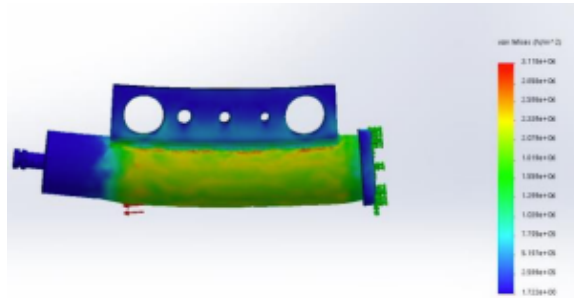


Figure 4.12: Nozzle stress analysis from SolidWorks

material was unchanged. Nevertheless, and taking advantage of new ProtoTherm nozzles that had been ordered, a couple of them were loaded and put in storage. Also, since the wall thickness was only .5mm, it was increased to 1.5mm to make the nozzle even stronger in case of creep.

After 15 weeks, the loaded ProtoTherm nozzles remained in good condition, and they were the ones with the original wall thickness of 0.5mm.



#### 4.8: Thermal Test

Using the new ProtoTherm nozzles, it was time for the thermal test. Because the vacuum chamber does not include thermal control, an oven and a freezer were utilized to perform the experiment. Thermocouples were used to monitor the temperature using a LabVIEW program. Two nozzles loaded with .6mL ink with HMPW, N44 with 2.04mm wax at the tip, and N46 with 1.92mm wax. Both were mounted on the metal plate, with only the metal rod guides holding the nozzles in place.

The test was performed to see the power draw of the burn wire at the extremes of the mission temperature ( $-40^{\circ}\text{C}$  to  $60^{\circ}\text{C}$ ). The information obtained would give the worst-case scenario of having to deploy the ink in an extremely cold environment. Conversely, in the hot environment, the wax would not take much time to melt, or would melt by itself. Overall, the effects of the wax plug in the two scenarios were observed. In orbit, the satellite would experience 45 minutes of sun and 45 minutes of shade, corresponding to the hot and cold environment respectively. In effect, 45 minutes was chosen per cycle. An oven and a refrigerator/freezer were used to conduct the experiment. The thermocouple was placed inside to help track and regulate the temperature as needed.

Both nozzles started the first cycle in the cold environment. Set to  $55^{\circ}\text{C}$ , the nozzles were introduced into the freezer and moved to the oven 45 minutes after. Within 5 minutes of being in

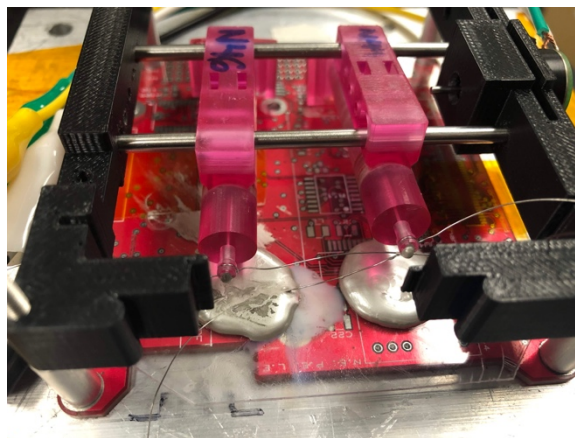


Figure 4.13: N46 (left) and N44 (right) deployed during hot thermal cycle

the oven, N44 failed, opening prematurely with a nozzle tip temperature of 41°C. At 11 minutes, N46 also failed, with a nozzle tip temperature of 53°C. For both nozzles, the wax melted prematurely and the ink deployed from the nozzle.

The test was repeated with nozzles N48 and N49. Both utilized the HMPW and were loaded with the same amount of ink. 4mm of wax were at the nozzle tip of N48, and 3.77mm of wax in N49. As much of the nozzle tip was covered with wax as possible. Again, the cycle started in the cold environment at -51°C. After only 30 minutes, the nozzles were moved to the hot environment. After 19 minutes, N48 failed at 60.13°C. A minute later, N49 failed at 60.65°C. Too close to the mission temperature, an alternative was sought.

In keeping with the wax concept, microcrystalline wax IGI 5909A with a melting point of 194°F (90°C) was used. Two more nozzles were used for the testing, N52 with 3.66mm of wax, and N53 with 4mm of wax. The same procedure was followed, except the nozzles went straight into the hot cycle to begin. Within 4 minutes, N52 failed at 45°C, and a minute later, N53 failed at 47°C. Although it has a higher melting point, the wax is considered soft and is mostly used as an additive. The wax did not really melt so much as became soft enough that the whole wax plug came out. Mixtures of the microcrystalline waxes were tested but all to no avail.

Once again, a roadblock had been encountered with the wax seal design and alternatives were started to be considered.

#### 4.9: Ink Cure Time

To determine the ink cure time for OF-2's primary payload, the experiment was conducted in high vacuum ( $\sim 10^{-5}$  torr), simulating running the experiment in space. A ProtoTherm nozzle was loaded with .6mL ink. HMPW was used for the seal, measuring at  $\sim 3.36$ mm inside the nozzle tip. 16mm of Nichrome wire was wrapped around the nozzle tip.

Connections to the motor and the test (printing surface) PCB were wired through a breadboard which is supplied power from outside the vacuum chamber. A microcontroller moved the motor which has been programmed to run the experiment as soon as the ink was deployed (visual confirmation only to start moving the nozzle). The burn wire was connected to an alternate power supply so that the time of deployment could be controlled. The setup of the printer and breadboard is seen in Figure 4.14.

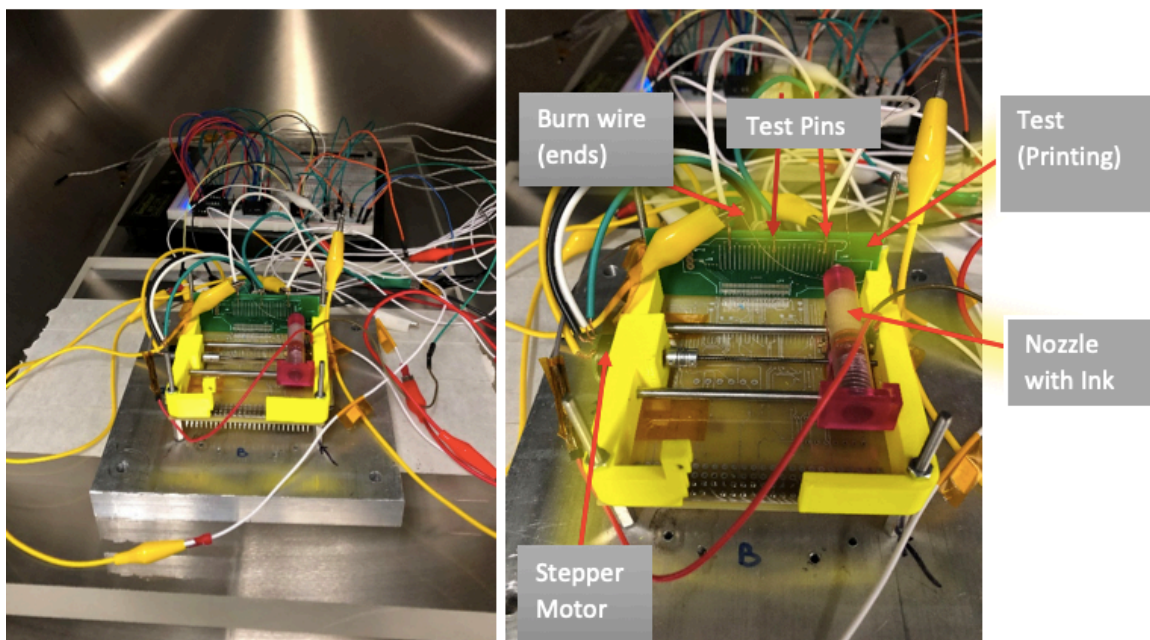


Figure 4.14: (a) Vacuum chamber test setup, (b) Printer close-up in vacuum chamber

To test the conductivity of the ink, the configuration in Figure 4.15 was used. As the Arduino was powered on before the ink cures, the output voltage reading from the conductivity test would read high, as the circuit was not yet closed. Once the ink cured, the circuit would close

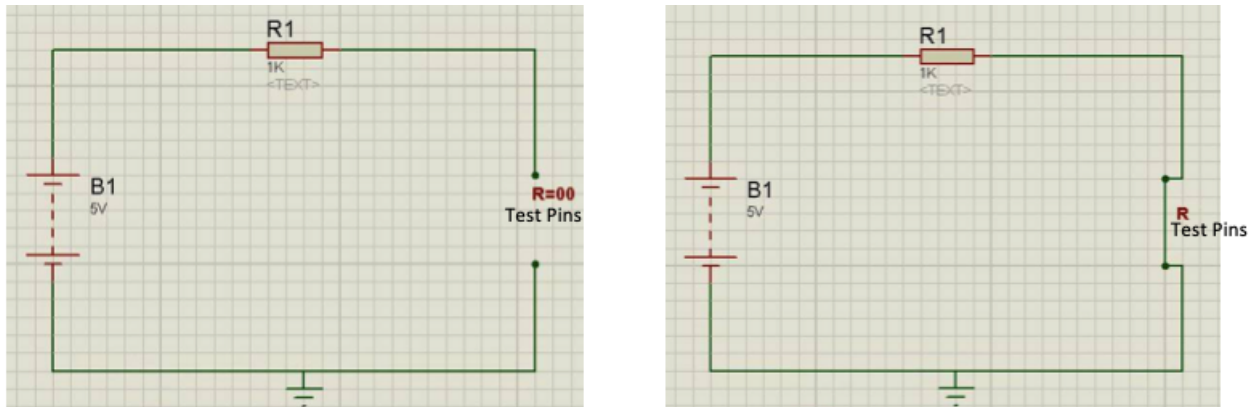


Figure 4.15: Conductivity test configuration (a) before the ink cures, and (b) after the ink cures

and the resistance would drop to zero, so the voltage output would drop towards zero.

After leaving the printer in high vacuum ( $\times 10^{-5}$ ) for an hour, the experiment was carried out. First the Arduino/breadboard was powered on to get ready to run the motor. The burn wire was activated and as soon as the ink started coming out, the motor sequence was started with the press of a button.

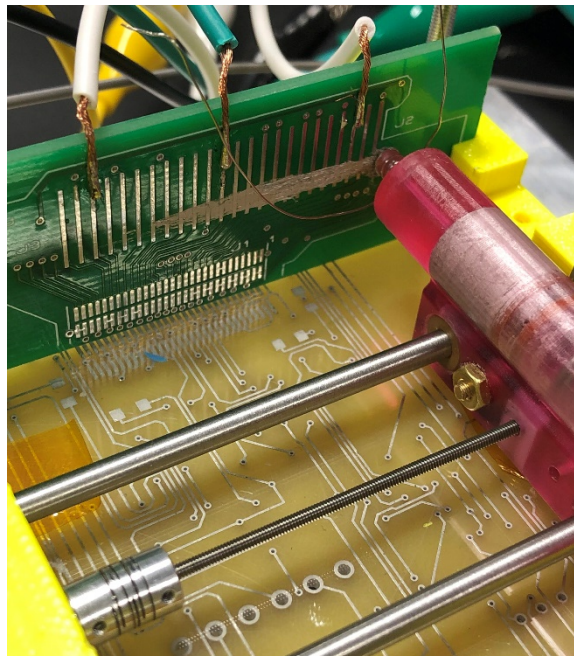


Figure 4.16: Ink trace deposition during ink cure time test in vacuum

The time when the conductivity test started was measured from when the trace of ink (from pin to pin, Figure 4.16) was deposited onto the test board. An initial voltage output of 3.87V indicated an open circuit. Within 65 seconds, the voltage output dropped below 3V, and within 90 seconds, the voltage output dropped below 2V,  $\frac{1}{2}$  the initial voltage output. After 152 seconds, the voltage output dropped to 1V. The graph below in Figure 4.17 shows the results of the experiment at the time the experiment was conducted.

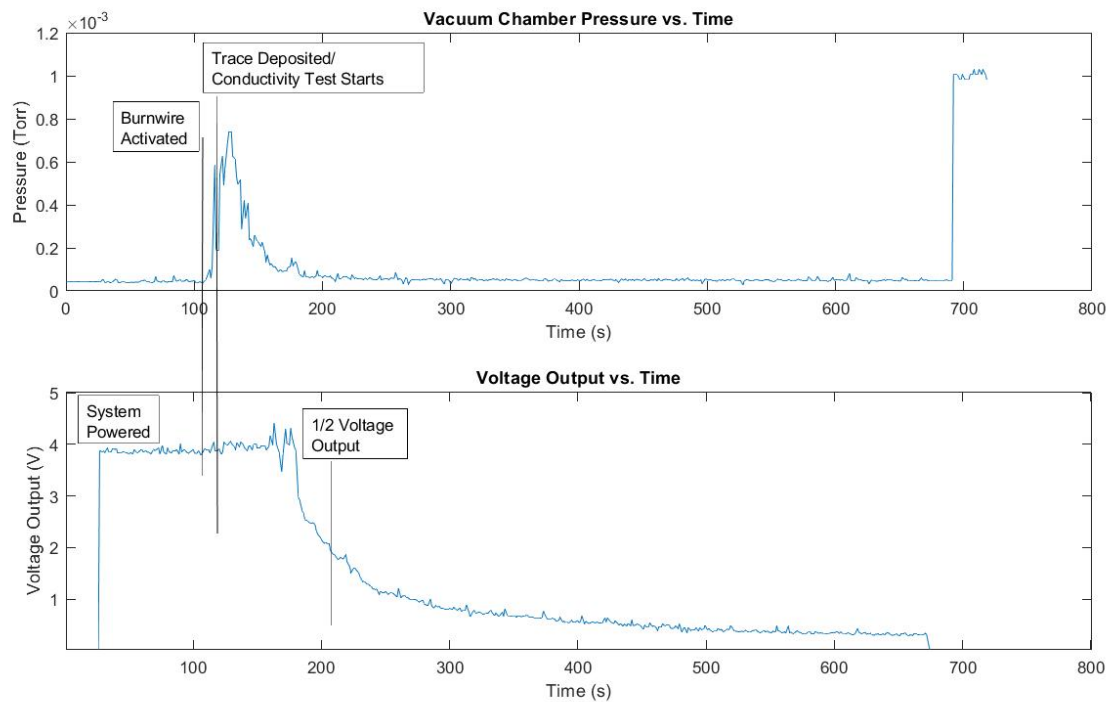


Figure 4.17: Ink curing time test data in vacuum

#### **4.10: Results**

Everything up to the thermal testing had worked, but with the possibility of the wax melting prematurely, the concept was at risk. Polyethylene wax has a higher melting point and is used in space applications, but it was difficult to find a provider that would sell small quantities. Solder was also considered, but with no metal components in the tip, the solder would not stick to the plastic. With the delivery deadline approaching, a decision had to be made.

## **Chapter 5: Solenoid Valve Nozzle Mechanism**

### **5.1: Solenoid Valve Nozzle Characterization**

Choosing a new design concept, a small solenoid valve was chosen. In essence, the valve would control the flow of the ink. The nozzle would be spring-loaded like in the previous designs. Also an NC valve, the nozzle remained closed until the valve was activated. A 2-port valve, it was compatible with the CubeSat due to its low power consumption (operating at 5V), it is small and compatible in size for the nozzle, and had flight heritage on CubeSats. By switching the polarity on the terminals, the valve could be either open or closed.

For material compatibility, two different combinations were available, Silicone internal seal with PPS plunger head, or Fluorocarbon (FKM) internal seal with PPA plunger head. Based on observation (since silicone O-rings were already used for the ink pusher, no reaction had been noted when in contact with the ink. In direct exposure with acetone (pure), the silicone could swell, eventually going back to its original shape once not in contact. It is considered ‘conditionally resistant’ to it. Although the conductive ink does contain acetone, the concentration was not enough to have caused any reaction with the silicone. On the other hand, the PPS material was compatible with acetone. For the other material combination, FKM was not recommended for acetone. Thus, the silicone/PPS combination was chosen.

With the drawings of the valve readily available, an updated CAD was done to print new nozzles compatible with it. A drawing of the design can be observed in Figure 5.1.

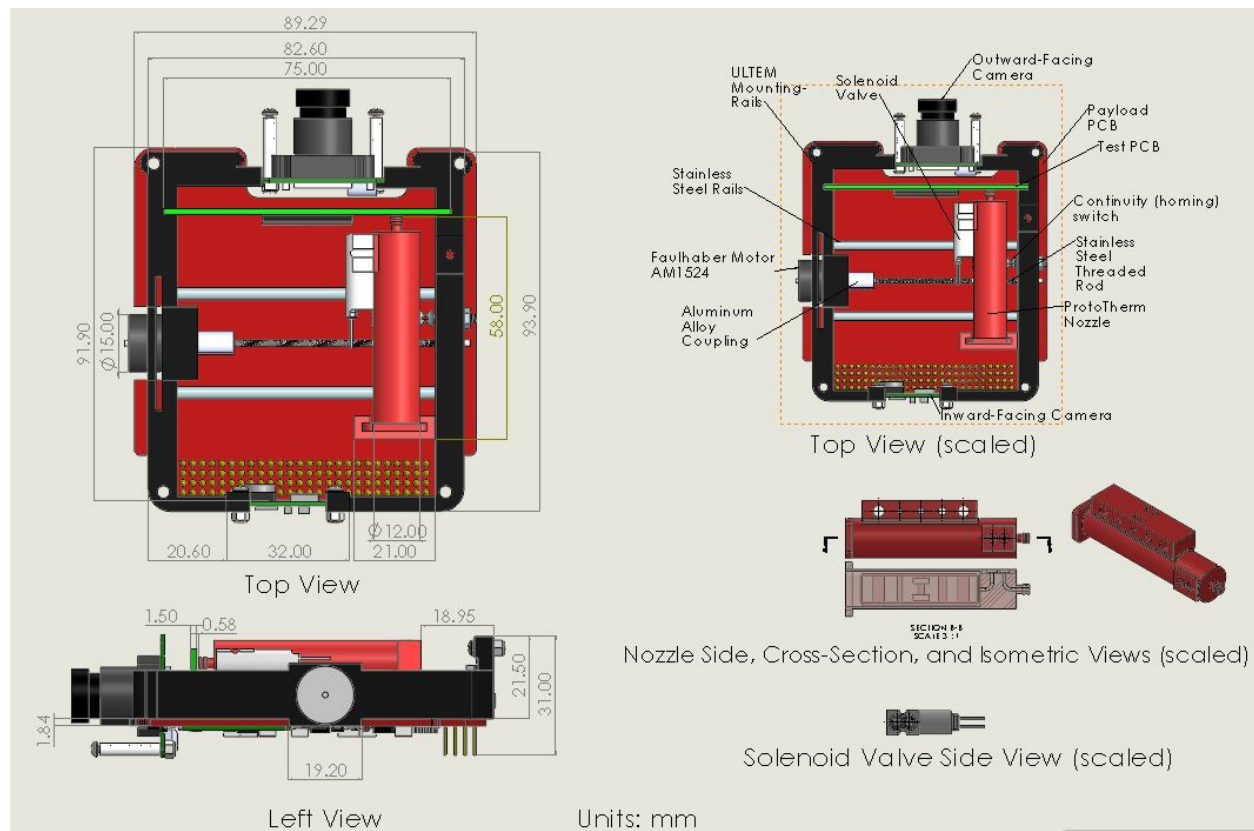


Figure 5.1: SolidWorks drawing of NC solenoid valve printer integration



## **5.2: Solenoid Valve Nozzle Characterization**

In previous designs, several nozzles would be printed and each one used only once due to the conductive ink being hard to wash off. With the valve, it was not possible to only use them once. Thus, for most of the testing, honey was used for testing. Although with different viscosities, honey had the closest consistency of the ink.

At the beginning, the valve mechanism was tested with water. There were no leaks even when pressurized. A momentary leak did occur from the nozzle mounting interface, however, it was due to the valve not being tighten hard enough on the nozzle. This was somewhat tricky as the valve mount was screwed into the nozzle, made of plastic. Too much force and the plastic cracked. Not enough force and leaks could occur. Testing with water helped to find leaks in the system, however, water dispenses much faster than more viscous substances, as expected.

Water was mixed with the honey to try to achieve the consistency of the ink. Three different nozzle designs were printed, each with different internal channels for the ink to travel to and from the valve. The small inter diameter was 1.3mm, the medium inner diameter was 1.9mm, and the large inner diameter was 2.05mm, corresponding to the size of the diameter on the valve channels. Comparing the previous design, the ink went from a large diameter where the ink was stored, to a small diameter at the tip. While the biggest channel diameter matched those of the valve and is good design practice to have them the same size, the contents were deployed fast. For the printer experiment this was not optimal as the nozzle would go back and forth to slowly deposit the ink on the test PCB. A pass from the nozzle (back and forth) onto the test PCB lasted about 27s. The results from the test indicated using smaller sized-channels was more beneficial.

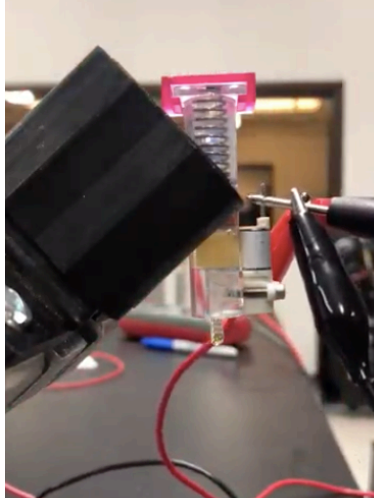


Figure 5.2: Functional testing setup of solenoid valve

### 5.3: Printer Dynamic Test

New nozzles were manufactured with an inner channel of 1mm and through several functional tests, were chosen as the final design. Using the alternatives to ink was beneficial since the components could be washed, dried, and reused. However, a printer dynamic test with ink was necessary to validate the function of the new nozzle. Done at atmosphere, the nozzle was loaded with 0.6mL ink and mounted on the printer assembly. As the valve was opened and the motor activated, ink started flowing and spreading onto the test PCB. Some running of the ink did occur as was usual of testing at atmosphere, however, previous tests with water also contributed to the ink ran off.

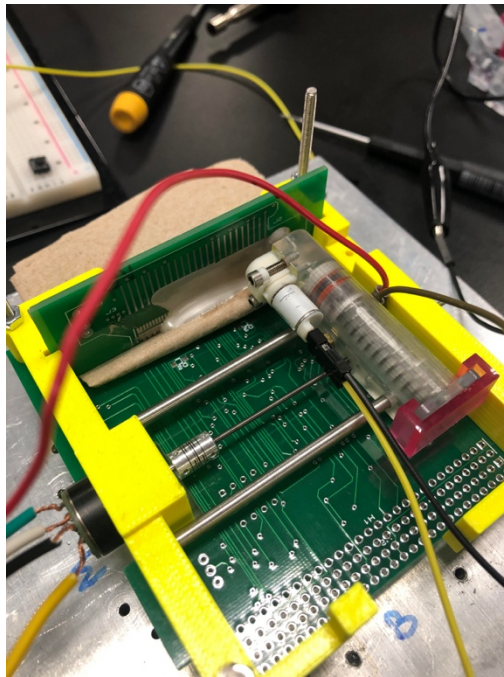


Figure 5.3: Final deposition of ink during dynamic functional testing

In the end, a weaker spring was also used. The final pressure exerted was  $\sim 24.63$ psi, and a nozzle with .9mm channels throughout was used based on testing results.

## 5.4: Printer Vibration Test

For the printer vibration test, a similar approach as that of the second design was used. Instead of using the honey, chocolate syrup was used because of its uniform consistency and similar behavior as that of the ink. A nozzle with 1mm channels was used, with the #4040 spring. Still, the .6mL amount of syrup was added. Except for the cameras, all the connections in the assembly were attached, with the other end of the connections taped to the aluminum base. An initial functionality test was first done, ensuring that the printer assembly worked before the test.

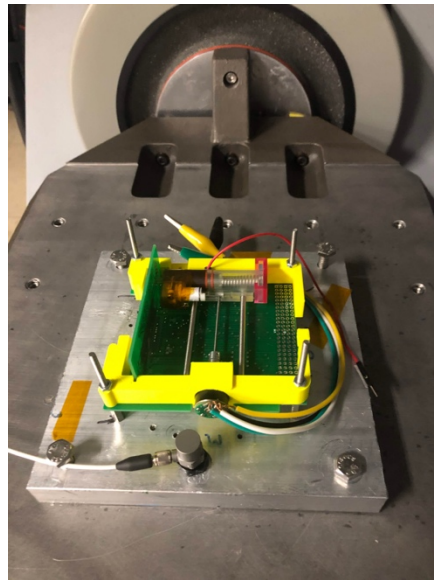


Figure 5.4: Nozzle assembly mounted on vibration table

Once again, the shaker table was run with the provided vibration profile. After being tested in two axes, the assembly was taken off the shaker table. Upon inspection, the motor had moved out a couple of millimeters. However, the motor would later be epoxied onto rail during final integration. As for the functionality test, the printer nozzle moved with no issues. Later, the valve was deployed to make sure the valve could still function, which it did.

## 5.5: Nozzle Thermal Testing

Knowing that the printer experiment could happen in a hot or cold environment, both scenarios were tested.

During the cold thermal cycle, a nozzle was placed inside the freezer, set to  $-53^{\circ}\text{C}$ . A thermocouple was placed on top of the valve. As the nozzle went from room temperature to an extremely cold environment, the nozzle was removed from the freezer at  $-40^{\circ}\text{C}$  before reaching a colder temperature. It was taken out and the power supply was used to open the valve. No syrup seemed to be coming out and the nozzle was left out. The ends of the power supply would be constantly touched to the valve terminals to see at what temperature it opened. Finally, at about  $13^{\circ}\text{C}$  the syrup was deployed.

A second test was followed, this time going to  $-30^{\circ}\text{C}$ . Immediately after taking it out of the freezer, the valve was activated, however, nothing came out. The nozzle was placed back in the freezer, ensuring the valve was closed. As the temperature quickly adjusted to room temperature, it was placed back in the freezer to  $-20^{\circ}\text{C}$ . When it reached the temperature, the nozzle was taken out and the valve was activated. Using the same method, the nozzle was left at room temperature and the valve was continually activated, until the nozzle deployed at  $16^{\circ}\text{C}$ .

Even though the valve could not be deployed in colder temperatures, the mechanism of the valve continued to work. The nozzle simply needed to warm to function again.

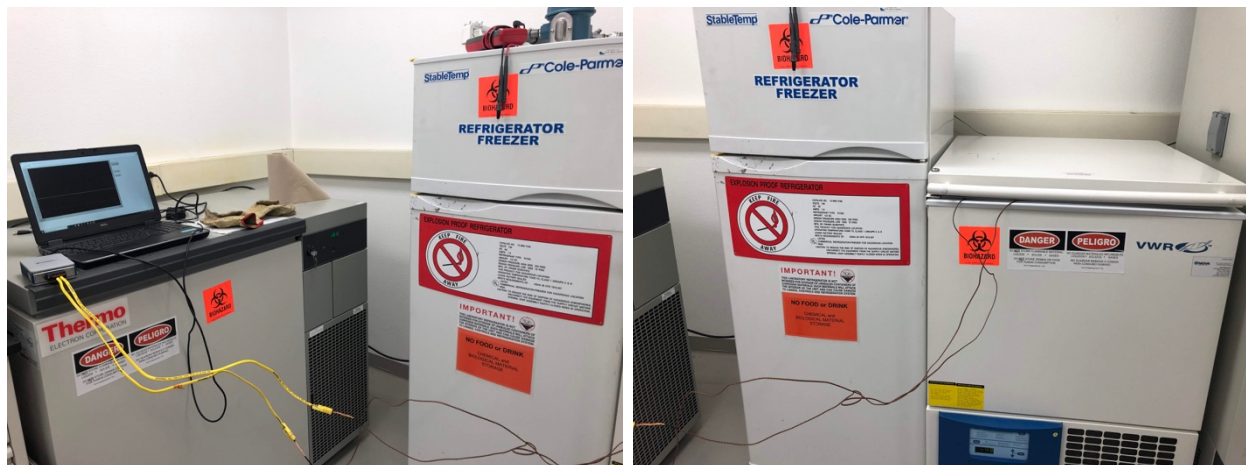


Figure 5.5: Cold thermal cycle setup with LabVIEW program monitoring temperature

On a different occasion, a different nozzle was subjected to thermal cycling. Starting in the freezer at  $-53^{\circ}\text{C}$ , the nozzle assembly was left inside for 45 minutes. After 45 minutes, the nozzle was moved to the oven at  $60-70^{\circ}\text{C}$ . A total of 3.5 cycles were completed, ending in the cold environment again. On the last cycle, the nozzle was removed from the freezer and placed inside the oven for the temperature to go up and stabilize. At  $10^{\circ}\text{C}$ , the valve could open and close using the power supply.

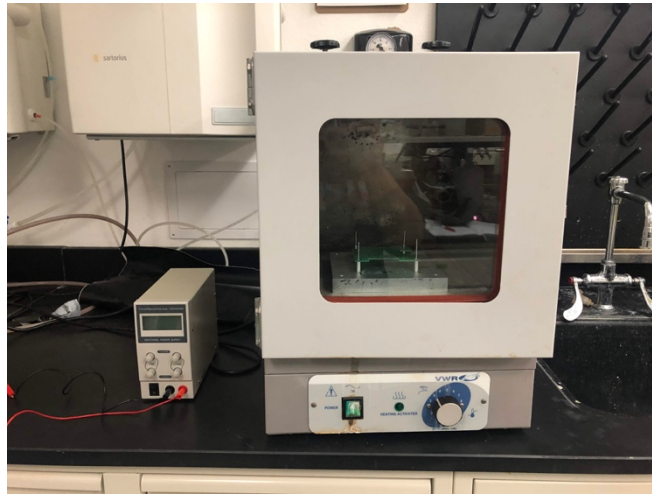


Figure 5.6: Hot thermal cycle setup

A temperature sensor was added to the printer assembly on top of the valve so that the OBC can first check the temperature before the experiment. If it is in cold environment, the experiment will not be conducted. With the programmed printer logic, the OBC will check at a later point until optimal conditions are reached.

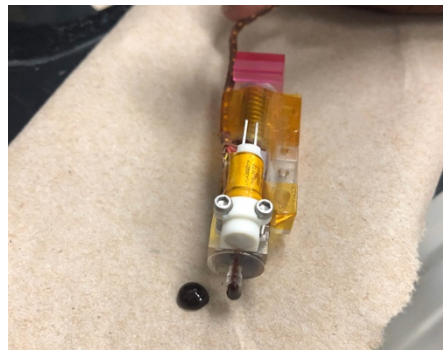


Figure 5.7: Nozzle starting to deploy after thermal cycling



## 5.6: Printer Vacuum Test

The last test needed was to run the printer inside the vacuum chamber. Since the goal was to ensure the functionality of the valve in vacuum, the nozzle assembly utilized was loaded with syrup instead of ink. A 1mm channel nozzle was used, loaded with .6mL of syrup. The complete printer assembly was mounted on the aluminum plate, with the motor connections wired to a breadboard where the microcontroller was also connected to the motor driver. On the outside of the chamber, two power supplies were used, one to power the microcontroller once in high-vacuum, and the other to power the valve.

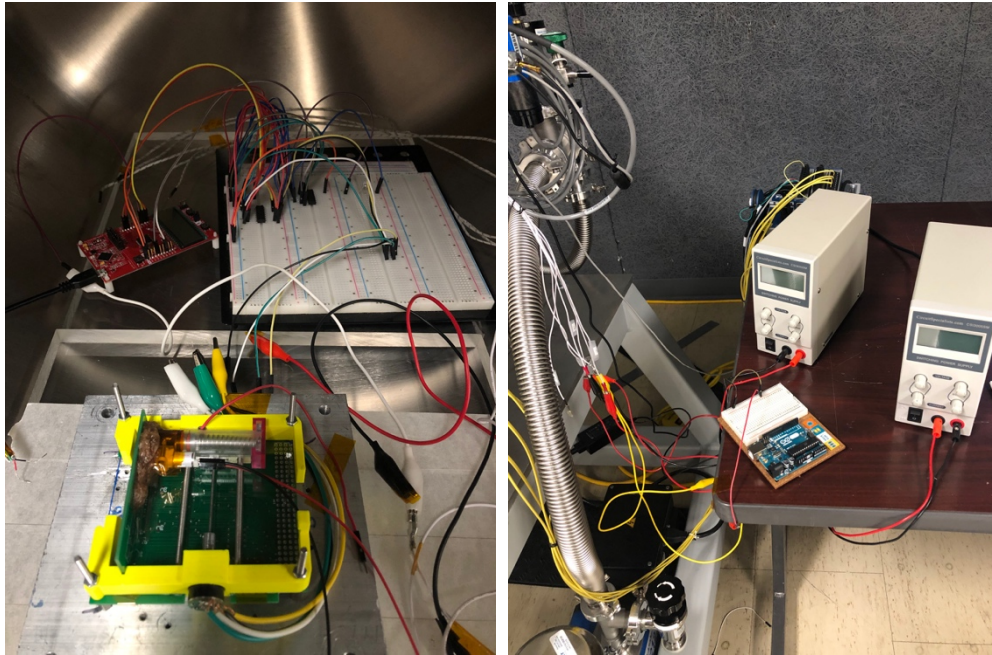


Figure 5.8: Vacuum chamber test setup (a) inside vacuum chamber, and (b) outside the chamber

Using the same procedures for previous vacuum chamber tests, the assembly and all components were placed inside. High vacuum was pulled to  $6.25 \times 10^{-5}$  torr and the test was carried. First, the power supply to the motor driver was turned on. Once the nozzle started moving, the valve was powered to open. Immediately, the syrup started coming out, indicating that the valve had worked as intended in vacuum.

## **5.7: Results**

Passing all the tests needed, the solenoid valve nozzle was the last design tasted and the one used for the OF-2 satellite. More testing could have been performed, to continue characterizing the assembly. Nevertheless, all tests were performed and were repeated on numerous occasions. At the end of the project once the structures team and the software team merged, the whole system was integrated and tested. No longer were external power supplies needed, or external microcontrollers. The printer assembly was tested until it was an autonomous system inside the satellite.

As of the writing of this thesis, OF-2 sits outside the ISS inside NanoRacks' CubeSat Deployer. In January 2020, the deployer will be raised into orbit, where the satellites will be released. Once in orbit, the real experiment begins.



## **Conclusion**

Orbital Factory 2 is UTEP's first CubeSat program to be planned, designed, and delivered for flight to LEO through NanoRacks, LLC. Initially winning a competition, the primary payload of the satellite aims to repair solar cells while in orbit, a proof-of-concept experiment housed inside a 1U satellite. A one-axis printer experiment will deposit a conductive ink trace on top of a test PCB that will become conductive upon curing, restoring the power to the cell system. Before flying, the printer experiment went through major design iterations to make sure it would be successful in space.

The first original design used a spring-loaded pin mechanism that blocked the flow of the ink inside the nozzle. However, several issues with leakage were unable to be resolved despite many efforts. With a new simplified design, the second nozzle design utilized a wax plug to contain the ink inside the nozzle. The downfall of that design, however, was the thermal test where the wax would melt prematurely and the ink would be deployed prematurely. As a last design, a small NC solenoid valve was mounted to the nozzle. Only when the experiment would be conducted, the valve would be opened, allowing for the ink to flow when required. In the three scenarios, similar tests were used to include: thermal, vacuum, and vibration testing. Thus, many of the procedures were repeatable, but they were all requirements that had to be met, and each design was tested to that. In the end, the last design was flown and now awaits to be performed in space sometime in January 2020 after it is deployed.

## References

- [1] D. Pignatelli "Poly Picosatellite Orbital Deployer Mk. III Rev. E User Guide". Rev. E. 2014
- [2] CubeSat Design Specification. Rev. 9. Retrieved from [http://org.ntnu.no/studsat/docs/proposal\\_1/A8%20-%20Cubesat%20Design%20Specification.pdf](http://org.ntnu.no/studsat/docs/proposal_1/A8%20-%20Cubesat%20Design%20Specification.pdf)
- [3] NASA's CubeSat Launch Initiative. Retrieved from [https://www.nasa.gov/directorates/heo/home/CubeSats\\_initiative](https://www.nasa.gov/directorates/heo/home/CubeSats_initiative)
- [4] Billah, Kazi Md Masum, "Characterization Of Electrically Conductive Inks In Simulated Space Environment" (2017). *Open Access Theses & Dissertations*. 413. [https://digitalcommons.utep.edu/open\\_etd/413](https://digitalcommons.utep.edu/open_etd/413)

## **Glossary**

CAD	Computer-aided design
COTS	Commercial off-the-shelf
cSETR	Center for Space Exploration and Technology Research
EPS	Electrical Power System
FDM	Fused-deposition modeling
GTO	Geostationary Transfer Orbit
HMPW	High melting point wax
I2C	Inter-integrated Circuit
LEO	Low earth orbit
LMPW	Low melting point wax
NASA	National Aeronautics and Space Administration
NC	Normally closed
OBC	On-board computer
OF-2	Orbital Factory 2
P-POD	Poly picosatellite orbital deployer
PCB	Printed circuit board
RBF	Remove before flight
SLS	Selective laser sintering
UART	Universal asynchronous receiver-transmitter
UHF	Ultra-high frequency
ULA	United Launch Alliance
UTEP	University of Texas at El Paso

## **Vita**

Perla Rocio Perez first attended Texas A&M University, where she received a B.A. in Mathematics in December 2013. She then returned home, where she was studying to take actuarial exams. With a change of heart, Perez decided to re-enroll for a second bachelors at The University of Texas at El Paso and pursue a degree in mechanical engineering.

In the 2.5 years it took her to earn a second bachelor's, she participated in a U.S.-Mexico Bidirectional Study Abroad on Program on Smart Cities. There, she participated in a Hackathon, with the opportunity to learn about developing phone applications and utilizing IBM Watson's services. She also had the opportunity to participate in the undergraduate research apprenticeship program (URAP) sponsored by the Army. There, she headed the additive manufacturing of hybrid two-dimensional layered materials and polymers.

After graduation, Perez knew she wanted to gain experience in the space field. Deciding to continue with a master's degree, she sought a research opportunity at UTEP's NASA MIRO Center for Space Exploration and Technology Research (cSETR), where she was hired. From the beginning, Perez was placed in the CubeSat team as part of the structures team. Working with the chassis structure at the beginning, she was later moved to the testing of the printer experiment. The efforts of all those involved in the Orbital Factory 2 CubeSat were seen when the satellite launched into space in November 2019. Through the center, Perez has been able to participate in different conferences, and has presented at the local Southwest Emerging Technology Symposium.

Perez had the opportunity to participate in a NASA internship at Johnson Space Center in Houston as a propulsion engineering intern. There, she worked on another CubeSat with a propulsion subsystem, and helped with the testing of the subsystem.

After graduation, Perez will work for Lockheed Martin Space. (perla.r.perez@gmail.com)